Polarization of Neutrons from the Photodisintegration of Deuterium*†

DAVID E. FREDERICK‡
University of Illinois, Urbana, Illinois
(Received 29 November 1962)

The polarization of neutrons photoproduced from deuterium at about 148° in the center-of-mass system was measured at four intervals in the photon energy range of 12.0–22.9 MeV in the laboratory system. The neutron polarization was analyzed in a low-pressure helium diffusion cloud chamber by scattering the neutrons and observing the left-right asymmetry in the helium gas nuclear recoils. This was achieved by photographing the individual recoils on film, then making measurements on the stereoscopically projected recoil track images, and finally subjecting the data to a maximum likelihood calculation. The flash photography of the random-scattering events was controlled by a photoelectric detection system: The cloud chamber was illuminated continuously with a slide projector light beam and a photomultiplier detected the reflected light from the formation of a densely ionizing track. The polarizations measured in the four photon-energy intervals of 12.0–12.9 MeV, 13.0–15.9 MeV, 16.0–17.9 MeV, and 18.0–22.9 MeV are -0.149 ± 0.100, -0.198 ± 0.086, -0.254 ± 0.120, and -0.295 ± 0.137, respectively. The polarization is defined to be positive in the direction of $\mathbf{k}_\gamma\times\mathbf{k}_{n0'}$ the directions of the incoming photon and outgoing photoneutron, respectively. The results are substantially in agreement with the polarization calculations by deSwart and Marshak and by Rustgi, Zernik, Breit, and Andrews.

I. INTRODUCTION

SINCE the photodisintegration of deuterium involves the transitions of the *n-p* system from the deuteron ground state to the continuum states by photon absorption, photodisintegration studies permit both another test of the best available nucleon-nucleon interaction models as well as the checking of the electromagnetic interaction itself. The ground-state Hamiltonian or wave function must predict the deuteron spin, parity, binding energy, and also the magnetic dipole and electric quadrupole moments. Simultaneously, the continuum final-state Hamiltonian or its eigenfunctions must predict the observed nucleon scattering cross sections. These Hamiltonians need not be the same if exchange forces are present. Below 100 MeV, there is no need to invoke mesonic effects and the electric interaction can be obtained from Siegert's theorem.[1] The magnetic interaction must be obtained by other means; usually the attempt is made to use a phenomenological prescription for it.

Presently available interaction models provide a good fit to the nucleon scattering cross sections and polarizations below 150 MeV.[2] Agreement in the photodisintegration situation also appears to be good except in the shape of the differential cross section in the 10–20 MeV range.[3,4] However, except near threshold, the $M1$ transitions contribute very little to the magnitude and shape of the photodisintegration cross section so it is desirable to find a circumstance where these transitions are important. Measurement of the polarization of the outgoing nucleons has been shown to provide such a situation. Theoretical calculations on photonuclear polarization were first made by Rosentsveig,[5] and Czyż and Sawicki[6] in 1956. Rosentsveig used a central force zero-range approximation. At higher energies, calculations have been performed using various nuclear models by Czyż and Sawicki, deSwart and Marshak, and by Rustgi, Zernik, Breit and Andrews.[3,4,7–10]

At 11–23 MeV, a range accessible to study by use of the Illinois 24-MeV betatron, approximately one-half of the nucleon polarization angular distribution, $P(\theta)$, is shown to be due to the pure $E1$ transitions and approximately one-half to the $E1$-$M1$ (spin flip) interference terms. Since the former is comparatively well understood, a first measurement of $P(\theta)$ can be considered to provide data on the latter.

The primary difficulty in measuring the photonucleon polarization from deuterium is the low event rate which is determined by the small photodisintegration cross section and the low scattering efficiency in the nucleon spin polarimeter. Since no relevant polarization measurements had yet been made at the start of the experiment, it was felt desirable to attempt a preliminary type of measurement of the neutron polarization in order to verify roughly the strength of the assumed $M1$ interaction and to look for any significant deviation from the expected results which are based on models

* This work was supported in part by the Office of Naval Research.

† This paper is based on a thesis submitted in partial fulfillment of the requirements for the Ph.D. degree at the University of Illinois.

‡ Present address: Department of Physics, Iowa State University, Ames, Iowa.

[1] See, for example, Robert G. Sachs, *Nuclear Theory* (Addison-Wesley Publishing Company, Inc., Cambridge, Massachusetts, 1953), p. 243.

[2] P. S. Signell and R. E. Marshak, Phys. Rev. **109**, 1229 (1958), P. S. Signell, R. Zinn, and R. E. Marshak, Phys. Rev. Letters **1**, 416 (1958).

[3] J. J. deSwart and R. E. Marshak, Physica **25**, 1001 (1959).

[4] M. L. Rustgi, W. Zernik, G. Breit, and D. J. Andrews, Phys. Rev. **120**, 1881 (1960).

[5] L. N. Rosentsveig, Soviet Phys.—JETP **4**, 280 (1957).

[6] W. Czyż and J. Sawicki, Nuovo Cimento **3**, 864 (1956).

[7] W. Czyż and J. Sawicki, Nuovo Cimento **5**, 45 (1957).

[8] W. Czyż and J. Sawicki, Phys. Rev. **110**, 900 (1958).

[9] J. J. deSwart, Physica **25**, 233 (1959).

[10] J. J. deSwart, W. Czyż, and J. Sawicki, Phys. Rev. Letters **2**, 51 (1959).

that provide good fits to the nucleon data and the photodisintegration cross sections.

II. EXPERIMENTAL METHOD

A. General

The neutron polarization from the photodisintegration of deuterium was measured at $146°\pm6°$ in the laboratory coordinate system for incident x rays in the energy range from 12 to 23 MeV. The spread in angle is calculated from the finite sizes of target and detector. Due to the low event rate, the data were grouped into four energy intervals. The Illinois betatron was used as a source of about 24-MeV electron bremsstrahlung produced at an internal fixed nickel target. A clean, narrow, and hardened x-ray beam was obtained by extensive collimation and shielding beyond a hardener of 3 in. of beryllium followed by 8 in. of paraffin. The beam was brought out 3.1 m from the betatron room into an external experimental area where it hit a target of liquid deuterium (see Fig. 1). The target, constructed in the style of Whalin and Reitz,[11] was essentially a cylinder 4 in. in diameter and 4 in. long coaxial with the beam. Its axis was aligned to within 2 mm of the beam axis and the effective photoproduction volume was 760 cm^3.

The transmitted beam was both monitored for integrated yield and stopped 10 m further in a paraffin and concrete pile. Since this was not an absolute experiment, quantitative yield measurements were only needed to normalize the data obtained from the various runs to permit background and bias subtractions. For this purpose, a Victoreen r-meter thimble was used.

The polarization was determined by the asymmetry in the right and left He(n,n) scattering.[12,13] The scattering events were detected by photographing the recoils

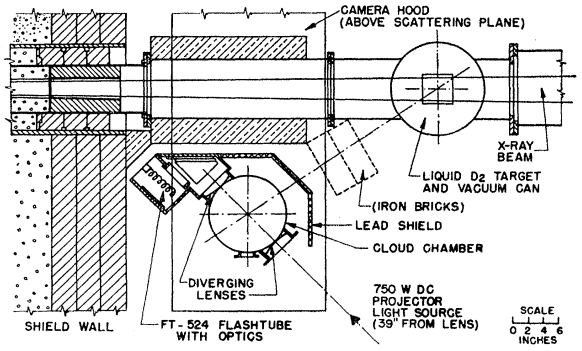

FIG. 1. General experimental layout. The betatron internal target was located 3.1 m to the left of the deuterium target. The precollimator block, the 12-in.-thick lead primary collimator, and most of the 48-in.-thick concrete and steel shield wall are not shown.

of the individual struck gas nuclei. Since they were doubly charged and four times heavier than recoiling protons from the hydrogen in the alcohol vapor, the He nuclear recoils could be distinguished by the more abundant vapor condensation on these more heavily ionizing tracks. Recoils from heavier contaminants were too short to be detected, due to the smaller energy transfer from the incident neutron. The photography of rare-random events was possible by triggering the photographic flash lamp by a photomultiplier circuit which detected the presence of vapor condensation occurring in the wake of a heavily ionizing charged particle in the chamber. The triggering scheme has been described elsewhere.[14] The events were stereoscopically recorded on film with two 35 mm cameras using the camera hood as described by Emigh.[15]

In order to measure the desired polarization, the amount of background, the asymmetry in the background, and the bias in the over-all experimental scheme, data runs were made under five different circumstances. The neutron background was composed of: deuterium neutrons which scatter into the cloud chamber from masses around the cloud chamber and the deuterium target, neutrons coming directly from the betatron and its beam collimator, neutrons from the x-ray beam path adjacent to the cloud chamber or from the x-ray beam stop, and also neutrons produced in the target holder which are not detected in run type 2 (see below) along with these other background sources. The conditions of the five run types along with the neutrons observed in each run were:

1. Target: Liquid deuterium in the target with the neutron flight path unblocked. The cloud chamber detected D(γ,n)H neutrons and all background neutrons.
2. Background: Deuterium in the target with $8\frac{1}{4}$ in. of iron bricks in the flight path (see Fig. 1). All background not coming from sources in the bricks' shadow was observed along with 3% of the attenuated D(γ,n)H flux.
3. Empty target: Empty target with unshielded neutron flight path. Only the background from the radiation shields, betatron room, and the x-ray beam was observed.
4. Empty target-iron: Run type 3 conditions with iron bricks in position. Background from beam and betatron only.
5. Pu-α-Be: Betatron off and deuterium target removed from vacuum jacket and replaced by a plutonium-beryllium neutron source inserted and centered at the deuterium position.

The Pu-α-Be source, a source of unpolarized neutrons with kinetic energies up to 10 MeV, is a fair

[11] E. A. Whalin, Jr., and R. A. Reitz, Rev. Sci. Instr. **26**, 59 (1955).
[12] Joseph V. Lepore, Phys. Rev. **79**, 137 (1950).
[13] John D. Seagrave, Phys. Rev. **92**, 1222 (1953).
[14] For a brief account, see David E. Frederick and J. H. Smith, Rev. Sci. Instr. **33**, 1100 (1962). The triggering and other experimental details are discussed more fully in David E. Frederick, thesis and University of Illinois Technical Report No. 34, 1962 (unpublished).
[15] C. R. Emigh, Rev. Sci. Instr. **25**, 567 (1954).

facsimile of the source of neutrons emanating from the x-ray-irradiated deuterium. Runs with it give combined information on asymmetries due to scattering of neutrons by room masses as well as any asymmetries in the detection equipment and/or film reading.

This is a low counting rate experiment. About 16 events per hour in the ranges of energy and angle desired were obtained in about 130 h of Target runs in the 11.0–22.9 MeV photon energy range. (The number of events above 23 MeV was only 26, because of the average betatron acceleration energy, hence they were ignored.)

The exposed Kodak Linagraph Ortho film was processed for development and then replaced in the cameras as before. Provisions were made to illuminate the film, thus converting the cameras to projectors. A pivoted projection apparatus replaced the target and cloud chamber detector equipment. It allowed spatial reprojection of the helium nuclear recoils and measurement of the range and angles of the recoils with respect to the neutron direction of flight, assuming that all the neutrons came from the center of the deuterium target. These data were used in simple digital computer calculations to determine the energy of the photon which produced the event and the detection efficiency of the helium scattering for an event of this kind. The events were grouped into energy bins and the deuterium polarization was statistically calculated by using the maximum likelihood method. Corrections were made for background and biases.

B. Cloud Chamber

The cloud chamber was located 75 cm from the deuterium target. Its internal volume was 6 in. high and 10 in. in diameter and was enclosed by a $\frac{1}{16}$-in.-thick stainless-steel wall. The chamber design and its clearing field operation were patterned somewhat after that described by Alston, Crewe, and Evans.[16] The two larger horizontal ports for chamber illumination and track photography are shown in Fig. 1. The light-diverging lenses also served to improve chamber stability near the wall by maintaining the vertical temperature distribution. However, the lens in the flash port concentrated the slide projector illumination in front of it by mirroring action. This diminished the sensitivity there. (The third port indicated in Fig. 1 was provided only for visual observation of the sensitive volume.) All port windows were made of Homalite CR-39 plastic[17] in order to eliminate all crazing, swelling and bulging of the windows. Though the top window had a useful diameter of 9.5 in., the alcohol trough size and the requirement for stereoscopic overlap of the two cameras' fields of view reduced the useful track-forming area to 280 cm^2, equivalent to a 7.4-in.-diam circle.

[16] M. H. Alston, A. V. Crewe, and W. H. Evans, Rev. Sci. Instr. **25**, 547 (1954).

[17] Homalite Corporation, Wilmington, Delaware.

Absolute methanol was used for the vapor source and could be supplied under pressure to the operating chamber from an external reservoir. The floor was cooled to 190–199°K by thermal conduction of heat down cooling fins to a liquid-nitrogen reservoir. The pressure was measured to 1% by use of a Bourdon gauge calibrated with a mercury manometer. The temperature in the chamber was monitored by three thermocouples located at the center of the floor, 10 cm above the floor at the wall, and in the alcohol trough. From measurements of the vertical and radial temperature distributions, these thermocouple readings provided knowledge of the temperature at any point of the sensitive volume with less than 3% error. Since helium behaves nearly like an ideal gas at low pressures,[18] the chamber temperature and pressure readings and a track's altitude in the chamber allowed a normalization of the track's length to that which would occur at standard temperature and pressure. Applying the available range-to-energy conversion data, we could calculate the alpha-particle recoil energies with about 5% uncertainty.

C. Run Data

The amount of data obtained is shown in Table I. The Background runs were interspersed with the Target runs. At their conclusion, the deuterium was evaporated and the two types of Empty Target runs immediately followed. With the plutonium source replacing the liquid target holder, the Pu-α-Be runs were made. Most Empty Target film frames were void of events because it was necessary to advance the film after about 25 sec to prohibit excessive film blackening by chamber floor reflections of the slide projector illumination. It is apparent that the film data efficiency was higher for the artificial neutron source runs than for the Target runs. Though its neutron flux-energy spectrum was quite similar to that for the D(γ,n) source, it was a somewhat more intense neutron source than the D(γ,n) reaction. Also, we discriminated more efficiently against proton recoil and short alpha-particle

TABLE I. Run data.

Run type	Total irradiation (arbitrary units)	Film and flash rate (seconds per event)	Number of film frames exposed (approx. only)	Number of useful events
Target	324.0	4.3	126 000	2093
Background	113.4	8.0	20 000	123
Empty target	34.9	19.	4100	8
Empty target-iron	36.9	19.	4100	7
Pu–α–Be	···	4.8	28 000	1775

[18] Dudley B. Chelton and Douglas B. Mann, Cryogenic Data Book, University of California Report UCRL-3421, 1956 (unpublished).

recoil events because we had only a limited supply of film remaining.

D. Film Reading

The cameras were so designed that the developed film could be both accurately repositioned in and projected with the same equipment.[15] To reduce the total scanning time required, film was also read on a second hood whose cameras were arranged to duplicate precisely the geometry of the first hood. Throughout the scanning, various checks were made to verify that the two reading hoods were optically identical and simultaneously congruent with the camera arrangement in the betatron run. The angle between camera axes was controlled to at least 0.2° and the image magnification was 1.00±0.01. The net effect of these misalignment uncertainties upon the photoneutron polarization was calculated to be negligible in comparison to the statistical uncertainties.

The projection device used was modeled on a design by Alston, Crewe, and Evans.[19] With this apparatus, when a track image was stereoscopically projected onto the rotatable and translatable plate, the alpha-particle recoil angle was equal to the angle between image direction and plate axis and the recoil azimuthal angle was equal to the plate rotation angle. The track length equaled the image length as measured on the screen. The construction included a device which allowed the height of the track above the cloud chamber floor to be measured.

The rms reading errors were controlled to 0.7° in recoil angle, 3° in azimuthal angle, $\frac{1}{2}$ mm in track length, and 1 mm in track altitude.

Since approximately half of the 180 000 frames of film had events of length greater than the minimum, it was necessary to select quickly those events for detailed study which were alpha-particle recoils into the desired solid angles stemming from photodisintegrations by photons of at least 12 MeV, the minimum desired photon energy. Allowed projected recoil angle and minimum range criteria were established to permit fast initial scanning of all frames by using the top camera view only. Approximately 18 000 events of all run types survived this first scan and they were then stereoscopically reprojected in order to make detailed measurements on them. This procedure allowed two-thirds of the scanning time to be devoted to these measurements. Approximately 8 000 events survived the second scan. A large fraction of the 10 000 rejected events were inclined more than 52° to the photoproduction plane, the angular limit which was set on the recoil azimuthal angle.

III. DATA ANALYSIS

A. Calculation of the Observed Polarizations

If the events due to photoneutron scatters to the left are grouped together and are N_L in number and N_R is the corresponding number of events due to right scatters, then the incident photoneutron flux polarization, P, is given by the left-right asymmetry:

$$P=\frac{N_L-N_R}{N_L+N_R}\frac{1}{\langle P_{He}(\theta_{n'},E_{n0})\rangle_{av}\langle\cos\phi_{n'}\rangle_{av}}, \quad (1)$$

where $\langle P_{He}(\theta_{n'},E_{n0})\rangle_{av}$ is the average neutron polarization resulting from the scattering of an unpolarized beam of neutrons of energy E_{n0} through a range of c.m. angles $\theta_{n'}$ and $\langle\cos\phi_{n'}\rangle_{av}$ is the value of the cosine of the scattered neutron azimuthal angle averaged over the recoil solid angle.[12] One can either calculate P with the above equation using the experimental values of N_L and N_R and the calculated values of $\langle P_{He}\rangle_{av}$ and $\langle\cos\phi_{n'}\rangle_{av}$ or one can form the likelihood function $\mathfrak{L}$ for the N total cloud chamber recoil events observed and obtain the photoneutron polarization by use of the maximum likelihood method. We used the latter method. The likelihood function for this experiment

TABLE II. Observed polarizations and numbers of events.

	Photon energy (MeV)	Recoil angle range	Likelihood estimates and numbers of events: Target[a]	N	Background	N	Empty target[b]	N	Pu-α-Be	N
	11.0–11.9	9.5°–30.5°	+0.059±0.070	347	−0.031±0.250	26	···		−0.025±0.07	364
	12.0–12.9	9.5°–30.5°	−0.117±0.078	276						
	13.0–15.9	9.5°–30.5°	−0.159±0.060	498	−0.016±0.304	19	···		+0.056±0.066	423
	16.0–17.9	9.5°–30.5°	−0.208±0.095	191	−0.042±0.341	14	···		+0.047±0.109	172
	18.0–22.9	9.5°–30.5°	−0.245±0.110	147	+0.66 ±0.56	7	···		+0.008±0.078	277
Av	11.0–22.9	9.5°–30.5°	−0.111±0.028	1459	+0.019±0.163	66	−0.45±0.5	6	+0.022±0.038	1236
	16.0–17.9	30.6°–50.5°	+0.085±0.098	325	+0.46 ±0.31	28	···		+0.000±0.125	200
	18.0–22.9	30.6°–50.5°	+0.144±0.094	309	−0.59 ±0.28	29	···		+0.172±0.09	339
Av	16.0–22.9	30.6°–50.5°	+0.115±0.068	634	−0.100±0.222	57	+0.1 ±0.5	9	+0.116±0.072	539

[a] These results are not yet corrected for background and bias.
[b] Empty target plus empty target-iron runs were combined.

[19] M. H. Alston, A. V. Crewe, and W. H. Evans, J. Sci. Instr. **31**, 252 (1954).

can easily be shown to be

$$\mathfrak{L} \equiv \prod_{i=1}^{N} \{1+P[P_{\mathrm{He}}(\theta_{n'},E_{n0})\cos\phi_{n'}]_i\}. \qquad (2)$$

The quantity P_{He} can be calculated for each event in terms of the neutron energy and scattering angle given the n-α scattering phase shifts.[12,13] Thus, no detailed knowledge of the photon energy spectrum, scattering cross section, and track sensitivity throughout the chamber which is needed in evaluating the average He(n,n) polarization in Eq. (1) is now required. To use the likelihood function, Eq. (2), it is sufficient that no left-right asymmetry occur in the neutron polarimeter and no left-right biasing enter the film reading. Even though the boundary of the useful camera overlap region was not symmetric about the average incident neutron direction, a recomputation of results using only those events which occurred wholly within a central, symmetric region of the cloud chamber—about 60% of the total number—showed that an upper limit on such a false polarization would be about 0.02 in magnitude. Any such breakdowns in the assumptions on which $\mathfrak{L}$ was predicated would also affect the results obtained from running with the unpolarized neutron source. The bias subtraction to be discussed below would correct for such effects.

The film reading data for each event was fed into a simple digital computer kinematics program which calculated both the energy of the incident photon and $P_{\mathrm{He}}\cos\phi_{n'}$, the statistical weight which described the helium detection efficiency for measuring each neutron's spin orientation. The calculated results for each event were placed on punched cards. As shown in Table II, the events were grouped by photon energy and recoil angle and the observed polarization was calculated by the maximum likelihood method for each run type. The photon energy intervals shown were not chosen to be equally spaced, but rather were chosen to reduce the spread in statistical uncertainties. Film-reading recoil angle limits had been set at a forward limit of 8° for all recoils associated with photons in the 12–24 MeV energy range and the rear limits of 32° for photon energies less than 19 MeV and 52° for photon energies less than 24 MeV. These film-reading limits resulted from a compromise among flash triggering reliability, accuracy of measurement on the reprojected tracks, and the polarization information content of the tracks at the different angles. For energies less than 19 MeV, the recoil path length was less than about 1.3 cm at the lab recoil angle of 52°; this occurred at the more forward angle of 32° for energies less than 12 MeV. Near this latter angle, the helium polarization changes sign. To eliminate possible biasing in the film reading at the extreme boundaries, the boundaries were later arbitrarily moved in 1.5 deg. So many 11.0–11.9 MeV events were found to have survived the film scanning that they were retained for further analysis. This resulted from the conservative minimum-range criterion which was used. Subsequent analysis showed that probably few of these events were rejected during the film reading. Similarly, events in the 16.0–18.9 MeV interval survived in number in the 32°–52° solid angle interval. They too were retained for some further analysis. For ease of background and bias subtraction, the two groups with $E_\gamma \geq 16.0$ MeV were split at the 30.5° recoil angle value and each pair of solid angle measurements was treated throughout the analysis as separate experimental measurements.

The uncertainties assigned to the polarizations tabulated in Table II are the standard deviations inferred from plots of the likelihood functions for each group. Figure 2 is a plot of the likelihood function for one of the smallest groups. The goodness of fit of a normal distribution to the calculated likelihood function was the justification for using the width of the likelihood function for the standard deviation of the observed (uncorrected) polarization.[20] Because of the meager amount of data, the Empty Target run events were not subdivided into photon energy groups. The data for 11.0–12.9 MeV were combined for the Background and Pu-α-Be runs. For the Pu-α-Be runs, photon energy is to be interpreted as the photon energy necessary to produce the same energy neutron in the D(γ,n) reaction as actually came from the $Be^9(\alpha,n)$ reaction within the plutonium source.

B. Data Checks

The deleterious effects of any bias in an experiment to measure a scattering asymmetry are obvious. Since n-p scattering is independent of spin at these energies,

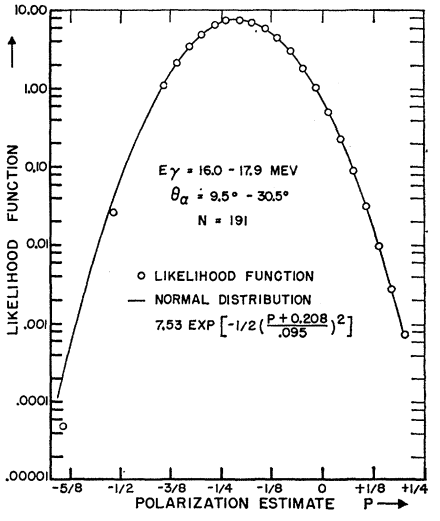

FIG. 2. Likelihood function for the observed photoneutron polarization for one of the recoil energy-angle groups containing the fewest number of events. The empirical smooth curve is a Gaussian distribution.

[20] H. Cramér, *Mathematical Methods of Statistics* (Princeton University Press, Princeton, New Jersey, 1946).

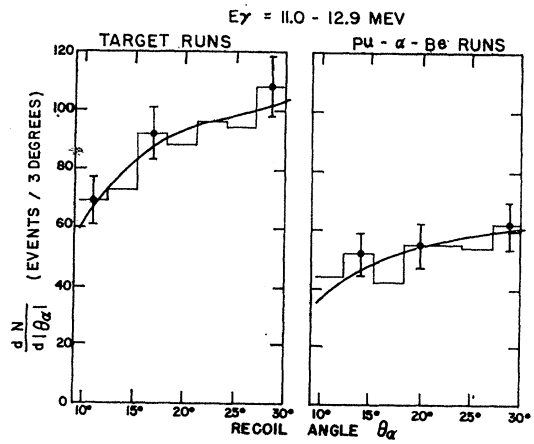

FIG. 3. Angular distributions of events for the combined 11.0–12.9 MeV photon energy groups. The smooth curves are the expected distributions normalized to the total number of events within each group. "Photon energy" as applied to recoil events produced in the runs with the Pu-α-Be source is defined in the text.

it is also important to be sure that the apparent differentiation made between proton and alpha-particle recoils was both valid and complete. The punched cards were used in many studies of reliability of the data with regard to these problems. Figures 3 and 4 show as histograms the angular distribution of events for the lowest and highest energy groups for the Target and Pu-α-Be runs. The error flags represent the statistical errors only. The smooth curves are the He(n,n) angular distributions, obtained from Dodder and Gammel's phase shifts,[13] normalized to the total number of events observed in each group. For the 18.0–22.9 MeV groups, the recoils were long enough to necessitate

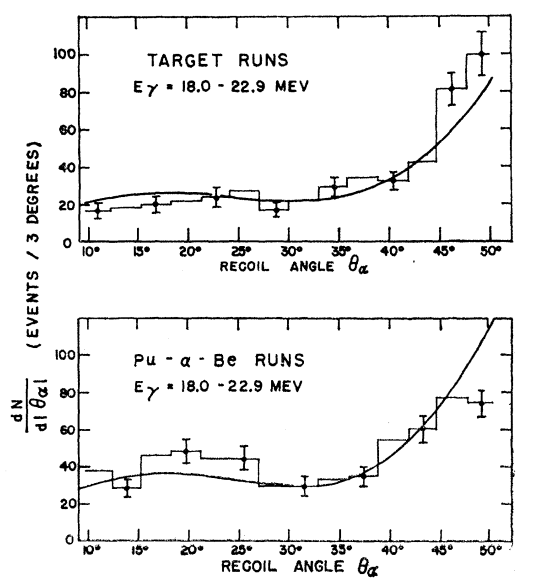

FIG. 4. Angular distributions of events for the highest photon energy group.

correcting the expected angular distributions for around 10% loss of events terminating beyond the top, bottom, or sides of the sensitive volume. Except for recoils back of about 45°, there is good agreement of the data with the expected distributions. The agreement is similar for the other two energy groups. The excess of events to the rear of 45° in the Target runs and the deficiency in the Pu-α-Be runs may be significant. These events are the shortest tracks in the chamber and therefore are the most difficult to trigger on and to reproject. Due to the great energy loss at low speeds, even the proton tracks deplete the chamber vapor supply at the end of the proton recoils. This caused great difficulty in differentiating between protons and alpha particles in these short recoils. Also, as noted earlier, a change in run operation was made for the Pu-α-Be runs. To reduce the waste film consumption, discrimination against short recoils was increased. This might affect the accuracy of background and bias subtraction for those energy-angle groups involving the shortest recoils. Since the corrections to the expected angular distributions were fairly well understood and because of the consistent high quality of the longer forward recoils, this interpretation is more credible than the inference that there was instead a very sizeable attrition of long, forward recoils in the target runs.

Another test for both bias in the application of the film reading criteria and proton contamination of the good events is the distribution of events by E_γ. Figure 5 shows the distribution for the target runs data as a histogram with the solid angles kept separate. The smooth curves are the expected distributions for both solid angles including corrections for beam hardening. They are normalized for the forward solid angle only. It can be seen that there was a sizeable loss, probably due to the minimum range film reading criterion, below 11 MeV but there seems to be no such loss apparent in the large-angle data near 16 MeV.

The dashed curve in Fig. 5 is the distribution expected had all the recoils been proton recoils. On the basis of these and other tests of the data, it was felt that the helium recoil data could not have been seriously contaminated with proton tracks. Further, other tests showed there was no polarization bias in any rejection of alpha tracks which might have appeared to be only lightly ionizing due to poor chamber sensitivity.

C. Background and Bias Subtractions

Since we did not choose to include background subtractions in the likelihood calculation, the deuterium photoneutron polarizations so calculated and listed in Table II need not be the true ones. For example, these likelihood estimates were derived using all events found in each group but some of the events were background events which should have been discarded while others were missing due to erroneous rejection. To correct for

background and biases, we used a modified box analysis scheme starting with Eq. (1). There are four possible "sources" of neutrons as is shown in Fig. 6. (A) The desired $D(\gamma,n)$ neutrons produced in the target. (B) Neutrons from photodisintegrations in the target which are subsequently scattered off walls, etc. [about 12% of (A)]. (C) Other sources: beam area, through the wall, from the beam stop, etc. [about 3% of (A)]. (D) Neutrons from the beam incident upon the radiation shields, target walls, and the condensate on the target walls [$\lesssim$1.5% of (A)].

Neutrons in the x-ray beam which scatter from the deuterium can be neglected because of their high momentum loss to the recoiling deuterons. The nondeuterium sources (C) and (D) are distinguished by the fact that flux (D) and not flux (C) is attenuated during runs with the iron shadow cone in place. Due to equipment layout, very few of the neutrons from source (B) will be in line with the iron bricks. The iron brick neutron transmission was 3%.

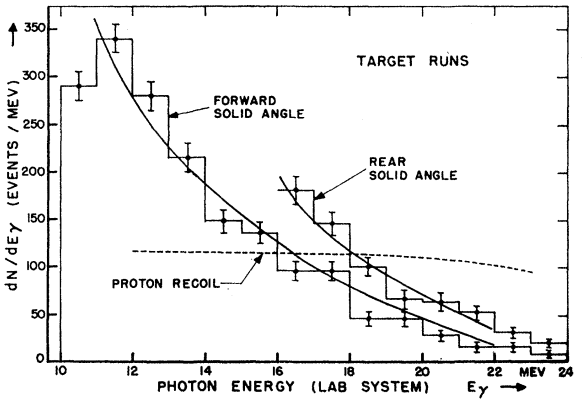

FIG. 5. Photon energy distribution for data runs with the deuterium target. The smooth solid curves are the expected alpha-particle recoil distributions, normalized to the observed number of recoils in the 9.5°–30.5° recoil-angle range. The dashed curve is the distribution expected had the recoils been due to neutron scattering by the hydrogenic constituent of the methanol vapor.

It was found that the effect of source (D) on the deuterium photoneutron polarization, P, was a correction term equal to the product of 0.015, the fractional amount present from this background source, and the apparent polarization of the neutrons from source (D). Since the source is roughly concentric with the deuterium target, the degree of polarization of this source should also be small. Therefore, this source is not considered further.

Neutrons from source (A) will preferentially scatter right or left because of their polarization—the effect which this experiment seeks to measure. Neutrons from (B) will *appear* to scatter preferentially right or left because they come from preferred points in the room, as will those from (C) also. In addition, there

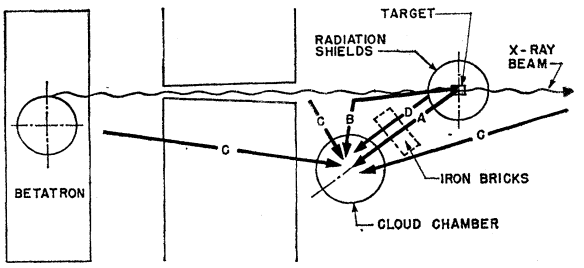

FIG. 6. The four sources of background neutrons.

may be biasing in the inefficiencies of detecting the recoils to left or right due to triggering, chamber sensitivity, and/or reader scanning.

It is a reasonably straightforward calculation to show that starting with equations of the form of Eq. (1) for the asymmetry measured in each different run type in terms of biased asymmetries from the different sources (A), (B), and (C), one gets a set of three equations which can be solved for the true $D(\gamma,n)$ asymmetry, the asymmetry from the so-called source (A).[14] Since the different types of runs had similar distributions for $\phi_{n'}$, θ_α (hence $\theta_{n'}$), and E_γ, the factor $\langle P_{\mathrm{He}} \cos\phi_{n'}\rangle_{\mathrm{av}}$ will be approximately the same for each run type. The final asymmetry equation then becomes an equation for the photoneutron polarization:

$$P=\left(1+\frac{B}{A}+\frac{C}{A}\right)P(\mathrm{D_2}) -\left(1+\frac{B}{A}\right)P(\text{Pu-}\alpha\text{-Be})-\frac{C}{A}P(\mathrm{MT}), \quad (3)$$

where $P(\mathrm{D_2})$, P(Pu-α-Be) and P(MT) are the observed polarizations in the target, Pu-α-Be, and Empty Target runs, respectively. B/A and C/A are the fractional amounts of background present from each of the two sources (B) and (C). Since the maximum likelihood method provides the observed polarization values $P(\mathrm{D_2})$, P(Pu-α-Be), and P(MT) with the least bias, we can use the results listed in Table II to substitute into Eq. (3).

This prescription for the background subtraction can be readily understood: For small right-left asymmetries in the backgrounds and biases, the polarization observed in any run is just a linear combination of these effects to a sufficient first order approximation. If there were no asymmetry in any of the neutron backgrounds nor any biasing, the *true* Target run neutron polarization would be diluted by the extra background counts occurring equally left and right. The correction factor to be applied to the observed target run measurement $P(\mathrm{D_2})$ is just $(A+B+C)/A$. The term $(C/A)P(\mathrm{MT})$ is the effect of "polarization" in the background not produced by scattered deuterium photoneutrons. The remaining term is, in part, a correction for the polarization of the deuterium photoneutron background which

TABLE III. D(γ,n)H polarizations and errors.

Energy (MeV)	Angle group	Photoneutron polarization	Major contributions to the total error $dP(D_2)$	dP(Pu-α-Be)	dP(MT)	dP_{He}	$dP_{Target\ pos.}$
11.0–11.9	Forward	+0.051±0.091	0.077	0.042	0.009	13%	0.02
12.0–12.9		−0.149±0.100	0.086	0.042	0.009	13%	0.02
13.0–15.9		−0.198±0.086	0.067	0.042	0.009	13%	0.02
16.0–17.9		−0.254±0.120	0.105	0.042	0.009	13%	0.02
18.0–22.9		−0.296±0.137	0.122	0.042	0.009	13%	0.02
16.0–17.9	Rear	−0.039±0.158	0.125	0.088	0.037	13%	0.02
18.0–22.9		+0.038±0.155	0.120	0.088	0.037	13%	0.02

comes from scattering in the shielding masses around the cloud chamber sensitive volume; the bulk of this term is the subtraction of the biases in the event detection chain from cloud chamber to film readers. The background fractions were calculated from the total number of events obtained during each run type, normalized by the total amounts of irradiation obtained in each run type, and were corrected for variations in dead time. No correction was found to be necessary for variations in the sensitive volume depth among the different run types due to changes in the radiation level at which the chamber had to operate.

There is no reason for believing that the various correction factors in Eq. (3) should be strong functions of energy, though some might be highly dependent on angle. Table II shows no statistically significant variation with energy of the ratio of background to target counts. The ratio B/A was, therefore, taken to be 0.0916 for the forward angles and 0.201 for the backward angles independent of energy. The number of Empty Target counts was insufficient to allow any energy differentiation, so C/A was taken as 0.0187 for forward angles and 0.074 for backward angles. Similarly, P(MT) was taken independent of energy. Its average values in Table II were used. The spurious "polarization" of the neutron source runs showed no significant energy dependence so the values of P(Pu-α-Be) used were the averages shown in Table II.

In this manner, Eq. (3) was used to correct the observed neutron polarizations shown in Table II. The final corrected values are shown in the third column of Table III.

The analysis used to get Eq. (3) also allows one to separate out the various sources of background and bias which give the experimental results of Table II. In particular, the correction term for bias was only 0.010 in magnitude at the forward angles, but was 0.190 for the backward angles. This biasing is statistically significant and may be linked to an asymmetry in the reprojection process. The accuracy of projection is dependent upon the sensitivity of relative image motion to rotations of the projection screen about its axis. Tracks to the "right rear" are roughly perpendicular to the plane containing the two camera axes. Recoil images to the "left rear" lie roughly in the plane containing the two camera axes. The relative sensitivity of adjustment is found to be severely different in the two cases. For "left rear" recoil images, rotation of the projection screen about its axis causes both camera images to change their separate polar angles, as measured on the screen, at nearly the same rate. Thus, a wide range of plate inclinations appears to give the same degree of image parallelism. The projection congruence had to be obtained by comparing the two image lengths. This difference in reprojection precision may have affected the acceptance and rejection of tracks at the 50.5° limit.

In principle, the subtraction of bias and background by the use of Eq. (3) should give the same polarizations for forward and backward solid angles. The actual presence of significant bias in the backward recoils leads us to suspect the backward data. In addition, it has been mentioned that the data shown in Fig. 4 show different behavior for the Target and Pu-α-Be run data at the rearmost angles. It is, therefore, with little surprise, but a great deal of regret, that we report that in the photon energy interval of 16.0–22.9 MeV, the photoneutron polarization measurement based on the forward recoil data was −0.272±0.091, whereas it was 0.00±0.111 based separately on those to the rear. All our observations and data checks attested to the reliability of the forward angle results. Due to all the difficulties with the data from the short recoil tracks in the rear solid angle, the final results given for the interval of 16.0–22.9 MeV do not include the rear solid angle measurements.

IV. ERRORS

The photoneutron polarization uncertainties include the statistical uncertainties in the measured asymmetries in the Target, the Pu-α-Be, and the Empty Target runs, and in the background counting rates. Also included are the uncertainties in the transmission of the iron shadow cone, in the helium scattering polarization and in the deuterium target positioning relative to the Pu-α-Be source position. Three uncertainties had individual magnitudes of 0.005 or less. The other contributions to the polarization uncertainty are itemized in the last five columns of Table III. The rms uncertainties in the stereoscopic projection were small enough

that their random nature did not require including an additional contribution to the overall uncertainties.

The combined effects of scattering and polarization of the photoneutrons by the $\frac{1}{2}$-in. lead shield between cloud chamber and deuterium target was quite readily calculated to reduce the polarization by (0.03 ± 0.03) times the photoneutron polarization. Polarization values in Table III were increased by this amount.

Neutron scattering inside the deuterium target is a sizeable effect. Since large-angle scattering involves large momentum transfer from the photoneutron to the recoiling deuteron, only those neutrons which have single-scattered into the cloud chamber through an angle of less than 30°–60°, depending upon energy, will be accepted as useful events. The $D(\gamma,n)p$ polarization at 148° c.m. is near the peak value so the net effect will be to contaminate the partially polarized beam with a flux of lesser degree of polarization. This effect was not included in the final results but was estimated to reduce the true polarization by around 10%. The measured polarizations presented here may may be low by as much as 0.02. This effect will be greater for the low-energy groups and may in part account for the decrease in observed polarization toward lower energies.

V. CONCLUSIONS

The results are shown in Fig. 7 along with the theoretical predictions by deSwart and Marshak[3] and Rustgi *et al.*[4,21] The energies at which this experiment was performed were well above the peak of the deuterium photodisintegration giant resonance so it is to be expected that the energy trend would be smooth between the 11.2- and the 22.2-MeV points. Therefore, there is substantial agreement with the calculations in the interval from 12 to 23 MeV.

The polarization in the lowest photon energy interval, 11.0–11.9 MeV, is not shown. Like the 16.0–18.9 MeV rear solid angle measurement, this value was based upon short alpha-particle recoil events saved *a posteriori*. Since the experimental result obtained from these marginal data differs so greatly from the polarization obtained in the next higher energy interval, the 11-MEV value is viewed to be of doubtful validity.

Thus, to within the uncertainties of this experiment, the polarizations measured in the 12–23 MeV energy range at the c.m. production angle of about 148.5°

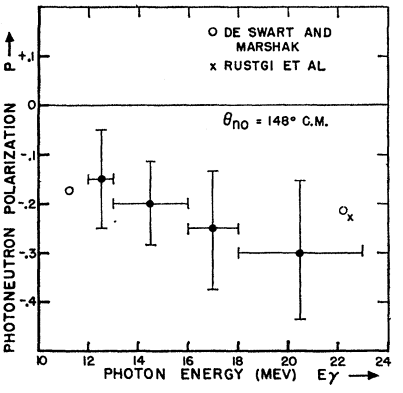

FIG. 7. Photoneutron polarizations measured in this experiment. The theoretical predictions at about 11 and 22 MeV are also shown.

support the *n-p* final-state interaction used. The magnetic dipole interaction used also appears to be of a reasonable magnitude, as was found earlier at 2.75 MeV by John and Martin.[22] In order to be able to calculate a better interaction potential by supplementing the available total cross section and angular distribution information with the polarization parameters, it will be necessary to improve the accuracy of these polarization measurements, as well as to measure the polarization angular distribution.

ACKNOWLEDGMENTS

I would like to thank Professor James H. Smith for his guidance and invaluable criticism throughout this experiment. I am indebted to Professor A. O. Hanson for suggesting this research problem and for obtaining the massive shielding and supplementary experimental space required. Professor L. J. Koester suggested the use of a diffusion-type cloud chamber.

The cooperation of Dr. A. V. Larson is gratefully acknowledged in maintaining continuous operation of the cloud chamber and in taking the data.

The author wishes to thank the many people involved in the various stages of this work: Mrs. Dorothy Carlson Lathrop constructed the deuterium target. L. D. Felts, R. G. Kinkade, and H. W. Moore conscientiously read film and helped in other phases of the work. A. M. Fenstermacher assisted in programming the calculations for the digital computer. The author very much appreciated and benefited from the cooperative support of the entire Betatron Laboratory Staff.

[21] W. Zickendraht, D. J. Andrews, M. L. Rustgi, W. Zernik, A. J. Torruella, and G. Breit, Phys. Rev. **124**, 1538 (1961).

[22] Walter John and Frederick V. Martin, Phys. Rev. **124**, 830 (1961).